

$z = 1$ multifractality of Swift short GRBs?

F. Tamburini

Università di Padova, Dipartimento di Astronomia, vicolo dell'Osservatorio 3, 35122 Padova, Italy
e-mail: fabrizio.tamburini@unipd.it

Received 14 January 2010 / Accepted 10 March 2010

ABSTRACT

Aims. We analyze and characterize the angular distribution of selected samples of gamma ray bursts (GRBs) from BATSE and Swift data to confirm that the division into two classes of short- and long-duration GRBs also correspond to two distinct spatial populations.

Methods. The angular distribution is analyzed using multifractal analysis and characterized by a multifractal spectrum of dimensions. Different spectra of dimensions relate to different angular distributions.

Results. The spectra of dimensions of short and long bursts indicate that the two populations indeed have two different angular distributions. Both Swift and BATSE long bursts appear to be homogeneously distributed across the sky with a monofractal distribution. In contrast, short GRBs follow a multifractal distribution for both the two samples. Even if BATSE data do not enable a unique interpretation of their angular distribution to be made because of the instrumental selection effects that mainly favor the detection of nearby GRBs, the results from Swift short GRBs confirm this behavior, also when including GRBs corrected by the redshift factor. The distributions traced by short GRBs, up to $z = 1$, depict a universe with a structure similar to that of a disordered porous material with uniformly distributed heterogeneous irregular structures, appearing more clustered than expected.

Key words. gamma rays: general – large-scale structure of Universe – chaos

1. Introduction

Gamma ray bursts (GRB) are catastrophic explosions of cosmological origin that illuminate the sky once or twice a day with relatively short, intense, flashes of γ -rays on the order of the MeV and duration that ranges from 10^{-3} to about 10^3 s. Until the launch of Swift, the most widely accepted taxonomy of GRBs had been the division between short-hard and long-soft bursts. In BATSE data, both Dezalay (1992) and Kouveliotou (1993) found a bimodal distribution in the burst duration, which was defined to be the time it takes the 90% of the flux to arrive (T_{90}) with respect to the local time of the detector. These two distinct GRB distributions are separated by a minimum located at $T_{90} \approx 2$ s. This sharp division is apparently also caused by a selection effect of the instrumentation onboard the satellite. New Swift observations permit us to include in the classification scheme, as short bursts, some distant events for which apparently $T_{90} > 2$ s with respect to Swift's proper time. The determination of the redshift allows us to correct the T_{90} for relativistic effects (Che et al. 1999; Ruffini et al. 2009). This suggests that a more solid classification of GRBs is required on the basis on a broader set of criteria, beyond the mere burst duration and the verification of the present taxonomy of long/short GRBs (Donaghy et al. 2006; Zhang et al. 2007; Bloom et al. 2008; Belczynski et al. 2008).

Long and short GRBs are understood to have been generated by different progenitors, which each contain a black hole that accretes material from either a disc or a torus with the emission of gamma rays (Ghirlanda et al. 2009). The basic model for long-duration GRBs, related to the catastrophic release of energy from the collapse of massive stars (Woolsey 2001; Fryer & Kalogera 2001), has received strong support from the observations of their X-ray (Gehrels et al. 2008; Nysewander et al. 2008), optical, and radio counterparts, and the association with supernova detections, of which the GRB980425/SN1998bw association was

the first clear example (Galama et al. 1998; Kulkarni 1998; van Paradijs 1999). Thus, X-ray flashes, which are associated to long-duration GRBs, are probably produced by the highly-relativistic jets ejected in core-collapse supernova explosions. The relativistic fireball model (Goodman 1986; Paczyński 1986, 1990; Castro-Tirado et al. 2001) provides a reasonable description of the observed afterglow spectrum, which is produced by the synchrotron emission of electrons accelerated in a relativistic shock with an estimated total energy budget roughly the same order of magnitude as that of supernovae Ib/c (Fraai 2001). The discovery of the slowly fading X-ray emission, from optical and radio afterglows of GRBs and the identification of host galaxies at cosmological distances provided additional support for their progenitors being produced short-lived massive stars at different cosmological epochs, whose detection is limited by the BATSE threshold to within distances slightly larger than $z \sim 4$ (Wijers et al. 1997; Blain & Natarajan 2000). The new data from Swift now has passed the barrier of $z = 8$ (Salvaterra et al. 2009).

Short GRBs are understood to be produced by highly – relativistic jets ejected during different processes, such as neutron star – neutron star (NS-NS) or black hole – neutron star (BH-NS) binary mergers (Narayan et al. 1992; Fox et al. 2005; Metzger et al. 2008), whose averaged redshift distribution, in the Swift-era, seems to be $\langle z \rangle \sim 1.0$ (see e.g., Magliocchetti et al. 2003; Tanvir et al. 2005; and Ghirlanda et al. 2006). Swift and HETE-2 observations have provided evidence of clear similarities with the afterglows detected in the correspondence of long GRBs, because of the detection of X-ray and optical afterglows (Soderberg 2006; Grupe 2006; Berger 2007). Other similarities identified in the spectra for the initial stage of short and long GRBs and the presence, in some cases, of X-ray flares infers that a common mechanism operates during the first few seconds (Barthelmy et al. 2005; Coward, 2007). Short GRBs have been observed mostly in elliptical galaxies, but

even less frequently also in nearby irregular and in star-forming galaxies, confirming as progenitor the binary merging scenario (Castro-Tirado et al. 2002; Mészáros 2006; Narayan et al. 2001; Belczynski et al. 2008) and the mechanism of *star swapping* are possible means of forming GRBs (Grindlay 2006). A similar behavior is expected for NS-BH binaries (Paczyński 1991). The angular and spatial distributions of BATSE GRBs appear to be isotropic (Briggs et al. 1996), there being only a few anisotropies in the angular distribution (Mészáros et al. 2000a,b,c). Short- and long- GRBs in the BATSE catalog actually show two different angular distributions (Vavrek et al. 2008; Balázs et al. 2009), but the connection to the hypothesis of the instrumental selection effect remains completely unclear.

In this paper, we characterize the angular distributions of the two classes of GRBs by performing multifractal analysis from a selected sample of BATSE and Swift observations, considering the redshift relativistic effects, and comparing the results obtained from the two catalogues. In Sect. 2, we describe the mathematical basis of our method. In Sect. 3, we estimate the fractal/multifractal dimensions by determining the distribution moments of the multifractal spectrum from the second up to the tenth order, and then draw our conclusions.

2. Fractal/multifractal analysis of the angular distribution

Being associated with galaxies, GRBs should trace the angular distribution of their host galaxies at distances slightly larger than those estimated with classical supernovae, i.e., distances on the order of a Gpc (Paczyński 1986; Usov & Chibisov 1975), across which inhomogeneity in the distribution of luminous matter should be averaged out on the Mpc scale.

Mandelbrot (1975) and Peebles (1980) used fractal geometry to describe the angular and spatial distribution of galaxies. They used Lévy-Rayleigh random paths, i.e., infinite-variance, stable, generalized random walks in which the step lengths are described by a tailed probability distribution. Galaxies are placed at the steps of a random walk and each galaxy is randomly connected with another in its vicinity, mimicking the random motion of a fly in the air. The power-law constraint of the motion determines the fractal exponent of the random path and rules the distribution of the jump lengths and the direction of each jump is taken isotropically at random (Martinez 2002).

Galaxy surveys show that the distribution of the luminous matter in the universe is more complicated than that of a single fractal. The distribution of galaxies has instead multifractal properties (Pietronero 1987; Célérier & Thieberger 2001), having a tendency to cluster following the well known peculiar structures produced by patterns of voids and filaments (Kurokawa et al. 1999). The CfA survey of nearby galaxies, for example, presents the scaling properties of these structures with a correlation dimension in the interval $D_2 \approx 1.3-1.4$. The two-point correlation function and the power spectrum analysis indicates that the distribution of galaxies on very large scales becomes homogeneous and isotropic like the X-ray background emitted by active galactic nuclei (AGNs), in agreement with the Cosmological Principle (Peebles 1993).

Multifractal scaling analysis has identified aggregated structures also in some samples of galaxies with distances larger than $r \sim 20$ Mpc. At scales larger than 30 Mpc, the angular distribution of luminous matter tends to homogeneity. According to Pietronero (1987), the distribution of luminous matter has multifractal properties with fractal dimensions that varies from

$d = 1.23$, for the nearby galaxies, up to the value $d \approx 2$ at very high redshifts. Multifractal distributions are usually present when a structure has different fractal dimensions on different parts of the geometric support; in other words, when spatial correlations are present and change the geometrical shape of the distribution on different scales (Falconer 1990). Those distributions cannot be adequately described by a geometrical support with a single fractal dimension, but require instead a whole spectrum of dimensions.

To characterize the angular distribution of GRBs in terms of multifractals, we use the “*method of moments*”, which estimates the fractality of the distribution by calculating the multifractal spectrum of generalized dimensions D_q in a given range (Falconer 1990; Feder 1988). If we consider N GRBs in a box of size L divided into cells of size r , the sample is said to have a non-null q th moment ξ_q on the scale r iff

$$\xi_q(r) = \sum_{i=1}^{L/r} \left(\frac{n_i}{N} \right)^q \neq 0 \quad \text{and} \quad (q > 2), \quad (1)$$

where n_i is the number of objects present in the i th cell. Higher moments reflect the emergence of structures present in the denser regions. From the scaling relation conducted on a two-dimensional section, we obtain (Kurokawa et al. 1999; Kurokawa et al. 2001),

$$\xi_q(r) \sim r^{(q-1)D_q} \quad (r_{\min} < r < r_{\max}), \quad (2)$$

where the coefficients D_q belong to the spectrum of generalized dimensions, D_0 is the *capacity dimension*, D_1 is the *information dimension*, and D_2 is the *correlation dimension*.

To estimate the multifractality of the distribution, one has to determine each generalized dimension $D - q$ as a function of the q th moment. One determines the dependence of each of the fractal dimensions on the moments by drawing the $q - D_q$ plot, which is based on the Lipschitz-Hölder exponent (Benassi et al. 1998; Goltz 1997). In the $q - D_q$ plot, one defines monofractals, those simple fractal structures described by only one dimension, D_f , and in the plot all the D_q s are equivalent to D_f . In the general case of a multifractal, instead, D_q usually decreases for higher and higher values of the moments q : if $q > q'$, then $D_q \leq D_{q'}$ until converging to the asymptotic value D_∞ for a distribution of infinite objects.

To characterise with high precision the multifractal distribution of a sample of objects in space, one usually does not need to calculate the generalized dimensions up to the limit dictated by the number of points in the space. For our purposes, a good estimate was obtained by taking $q = 10$ as an upper limit.

3. Results and discussion

From Swift observations, we selected a sample of 444 GRBs that do not have ambiguous classifications, 53 of which are classified as short-GRB after correcting of T_{90} for the relativistic effects (data updated at 2009-09-15). From BATSE 4 catalogue, instead, the total number of GRBs used in our analysis is 1843, 1447 of which are classified as long-GRBs.

To verify whether the classification into the two subgroups corresponds to two distinct populations in both the sets of data collected by BATSE and Swift, we also performed a series of tests of the angular distributions in different subsamples. We randomly selected from our data a sets of either short or long GRBs, mixed together, and then tested whether GRBs might be discriminated without choosing “a priori” the two classes following the

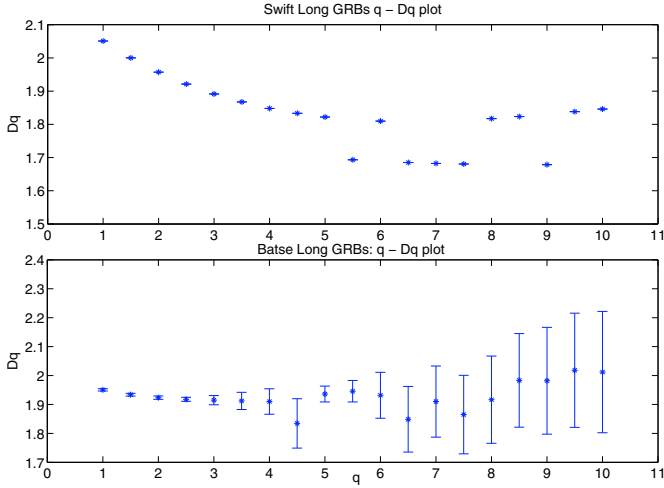


Fig. 1. *Upper panel:* $q - D_q$ plot of Swift *long* GRBs. The long bursts follow an angular homogeneous distribution. The moments D_q tend to decrease slowly from $D_1 \sim 2$ to $D_q \sim 1.8$ with a rise of the fractal dimension after $q = 8$. The spectrum of dimensions is that of a two dimensional Brownian motion with fractal dimension 2. *Lower panel:* BATSE 4 long bursts also exhibit a very similar homogeneous structure with a mean fractal dimension $D \approx 1.98$.

burst duration-time distribution. The two classes of long/short GRBs were distinguished by the fractal analysis of their angular distribution in the sky. More precisely, by progressively mixing the population of short GRBs with a growing sample of randomly chosen long GRBs, the multifractal dimension converged to that of a homogeneously distributed monofractal with dimension $d = 2$. This simple test corroborated the true subdivision of GRBs into the two short/long populations identifiable from both the BATSE and Swift data and also when the two datasets are mixed together.

We now present and discuss the results obtained for each different class of GRBs.

3.1. Long bursts

Figure 1 clearly shows the uniform angular distribution of both the samples of Swift and BATSE 4 selected data. The sample of data from Swift shows a homogeneous distribution. In this case, the moments D_q tend to decrease slowly from $D_1 \sim 2$ to $D_q \sim 1.8$ and the fractal dimension begins to increase after the moment $q = 8$. In the plot, we also present some sporadic and discontinuous jumps down to $D_q \sim 1.7$ that deviate from the main smoothness, a behavior that might be caused by numerical errors in the determination of certain D_q 's. In any case, this does not affect the interpretation of the global behavior observed in the plot. We observed a typical example of a stochastic homogeneous distribution, similar to that of a fractional Brownian motion (FBM) of dimension $D = 2$, which is expected from distant sources that homogeneously distribute according to the Cosmological Principle. The errorbars of the D_q 's are calculated from the error propagation of the statistical uncertainty in the position of each GRB and from the instrumental errors. In the case of Swift data, errorbars are too small to be visible in the graph.

By analyzing BATSE data, we observed a different behavior in the interval $4 < q < 6$, where the distribution is flat, within the experimental errors, and the angular distribution is characterized by an almost constant fractal dimension that fluctuates within the interval $D_q = [1.8-2]$ approximately describing the angular

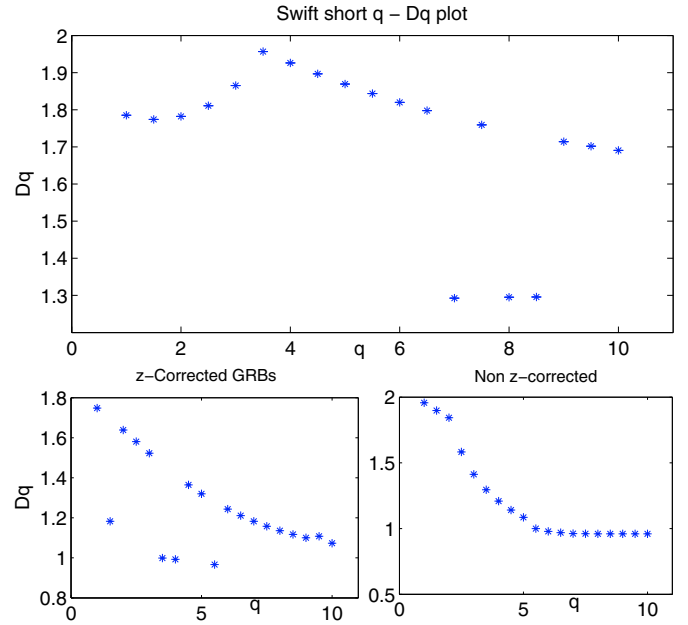


Fig. 2. $q - D_q$ plot of Swift *short* GRBs. *Upper panel:* spectrum of fractal dimensions of the angular distribution of the whole sample. This behavior with a maximum around $q = 3$ clearly indicates a multifractal homogeneous distribution very close to that of a multifractal Brownian motion. *Lower left panel:* dimension moments of the 13 z -corrected GRBs with relatively high redshift. The structure is clearly multifractal. *Lower panel:* the subsample of GRBs with already $T_{90} < 2$ s, exhibits a multifractal distribution, but with an asymptotic convergence to $D_q = 1$. In this case, the structure traced by the GRBs appears to be more clustered.

distribution of a uniform structure. We found a similar result in both the datasets, the redshift scale being around the Gyr (as confirmed by the redshift values obtained for most of the bursts), that is, long GRBs are distributed according to the Cosmological Principle, in which the Universe is completely homogeneous and isotropic on large scales.

3.2. Short bursts

They represent a more complicated set of phenomena with many unknown properties. Figure 2 presents data for the whole sample of 53 Swift short bursts in addition to the apparently-long bursts corrected by z and those with T_{90} already below 2 s. The sample is characterised by a spectrum of dimensions that decreases for increasing q 's, the signature of a multifractal distribution.

Short GRBs appear to be regularly angularly distributed because they follow multifractal Brownian motion (mBM) of mean index $H = 0.68$, a distribution that begins with a clustered shape then evolves towards homogeneity on relatively larger scales. The mBM is an extension of the fractional Brownian motion in the sense that the path regularity can vary with time, as observed during the evolution of anomalous diffusion processes. The Universe traced by short GRBs exhibits a multifractal structure, which presents non null autocorrelation on lower scales and evolves to homogeneity at larger distances. This structure appears to be similar to a disordered porous material that exhibits a heterogeneous structure, or even an irregular one in a uniform sense. This type of foam contains multiple, nested natural length scales or continuously evolving scales, while moving to higher redshifts (Lim & Muniandy 2002).

The differences between the distributions of short and long bursts, as evident in the plots, is confirmed by the correlation coefficients and the p -values obtained by comparing the results of averaging 10 sets of 53 randomly chosen (without repetition) long GRBs with respect to the total sample of short ones. The effects of the numerical problem that produced some outliers (e.g. the points at $D_q \sim 1.7$ in Fig. 1, upper panel) were corrected by applying a polynomial fit to the general trend. The correlation coefficient indicates the strength and the direction of a linear relationship existing between two data records. When there is a strong correlation, the correlation coefficient is $R \sim 1$, when there is no correlation, $R = 0$, and when an anti-correlation is present, $R \sim -1$. In general, a correlation greater than 0.8 is considered a strong correlation, whereas a correlation less than 0.5, is weak. The p -values are instead calculated to test the hypothesis of no-correlation, which is the probability of obtaining a correlation as large as the observed value by random chance, when the true correlation is zero. If the p -value is less than 0.05, one rejects the null hypothesis and the correlation R is significant (Wall & Jenkins 2003). For Swift data, long and short bursts have a very weak correlation ($R = 0.2656$) and a very low p -value of $p = 0.2868$, which rejects the no-correlation hypothesis. From Swift data, short and long GRBs seem to follow two independent angular distributions.

The further division of short GRBs into two sub-classes, one containing the short GRBs corrected for the redshift and the other containing only those GRBs that already present a T_{90} already below the 2 s, show that the two subsamples follow two mutually exclusive multifractal distributions and that the subclass of the z -corrected short GRBs has a higher fractal dimension q_0 , close to that of a homogeneous distribution, confirming the behavior expected from a mBM (see the two lower panels in Fig. 2).

The whole sample of BATSE short GRBs exhibits a spectrum of the general dimension D_q , smoother than that of the whole sample of BATSE long GRBs, as reported in the upper panel of Fig. 3. The capacity dimension D_0 and the correlation dimension D_2 have similar values close to $D_q \simeq 1.9$ which are smaller than those of long GRBs. This demonstrates that short GRBs have a different multifractal and more clustered distribution than to long ones. This difference is more evident if BATSE GRBs are divided into the two subclasses indicated by Mukherjee et al. (1998): Class II with short/faint/hard bursts and Class III with intermediate/intermediate/soft bursts (we recall that Class I correspond to long GRBs), as drawn in the lower panels of Fig. 3. Here, the generalized dimension D_q of both II and III classes alone indicates that the angular distribution is clearly multifractal, similar to that seen in the galaxy distribution at low redshifts.

By applying the same statistical test used to quantify the distributions in Swift data, the R and p values of BATSE data are found to be $R = -0.0741$ and $p = 0.7702$ which have slightly different statistical behavior: almost no (anti)-correlation with a high p -value. This is a clear indication of instrumental selection effects.

In conclusion, even if R and p values of BATSE data could be ascribed to a selection effect, Swift results confirm the existence of two different angular distributions associated with the two classes of short and long GRBs. In both Swift and BATSE data sets, long bursts are homogeneously angularly distributed. In contrast, short GRBs trace a distribution that appears to differ from that expected for the clustering of luminous matter in the Universe around the redshift value $z \sim 1$. We can clearly see a multifractal distribution in a structure that should already be

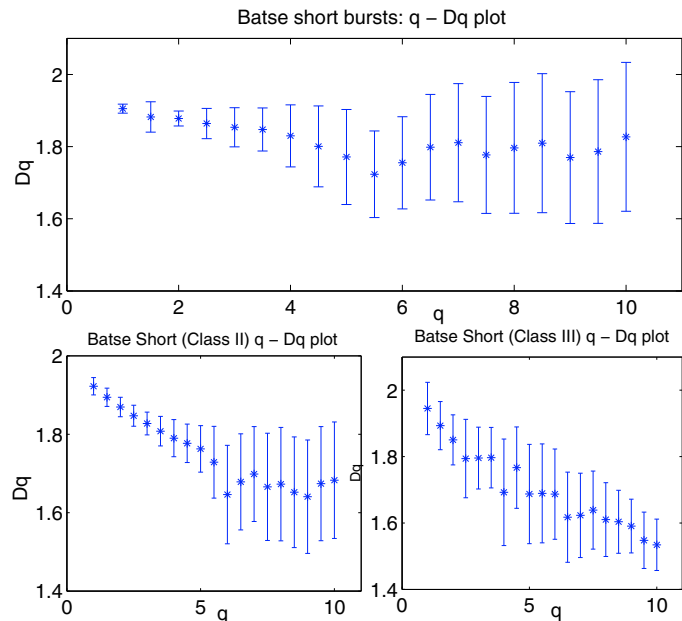


Fig. 3. Upper panel: $q - D_q$ plot of BATSE 4 short GRBs (Class I + Class II) exhibit a fractal structure with dimensions fluctuating around the value ≥ 1.8 . Lower left and right panels: $q - D_q$ plots of BATSE 4 short bursts, in which Class II and Class III, respectively, clearly follow a multifractal distribution.

homogeneously-distributed. By taking into account that the candidate progenitors of short GRBs probably migrate away from their initial positions, we should also expect an additional convolving effect on the detected structure that may tend to make the distribution more towards the total homogeneous, a result that has not been observed. This suggests either that GRBs are not good tracers of the matter distribution or that the Universe traced by GRBs appears more clustered at redshifts $z \lesssim 1$ than expected.

Acknowledgements. The author would like to acknowledge Massimo della Valle for the helpful discussions and suggestions.

References

- Balázs, L. G., Horváth, I., Vavrek, R., Bagoly, Z., & Mészáros, A. 2008, AIPC, 1000, 52
- Barthelmy, S. D., Chincarini, G., Burrows, D. N., et al. 2005, Nature, 438, 994
- Belczynski, K., Hartmann, D. H., Fryer, C. L., Holz, D. E., & O'Shea, B. 2010, ApJ, 708, 117
- Benassi, A., Cohen S., & Istas, J. 1998, Proba Lett., 39, 337
- Berger, E. 2007, ApJ, 670, 1254
- Blain, A. W., & Natarajan, P. 2000, MNRAS, 312, L35
- Bloom, J. S., Butler, N. R., & Perley, D. A. 2008, AIPC, 1000, 11
- Briggs, M. S., Paciesas, W. S., Pendleton, G. N., et al. 1996, ApJ, 459, 40
- Castro-Tirado, A. J., Sokolov, V. V., Gorosabel, J., et al. 2001, A&A, 370, 398
- Castro-Tirado, A. J., Castro Cerón, J. M., Gorosabel, J., et al. 2002, A&A, 393, L55
- Célérier, M.-N., & Thieberger, R. 2001, A&A, 367, 449
- Che, H., Yang, Y., Wu, M., & Li, Q. B. 1997, ApJ, 483, L25
- Coward, D. 2007, New Astron. Rev., 51, 539
- Dezalay, J.-P., et al. 1992, in Gamma-ray bursts; Proceedings of the Workshop, Univ. of Alabama, Huntsville, 304
- Donaghy, T. Q., Lamb, D. Q., Sakamoto, T., et al. 2006, unpublished [arXiv:astro-ph/0605570]
- Falconer, K. J. 1990, Fractal Geometry, mathematical foundations and applications (Brisbane (UK): Wiley & sons)
- Feder, J. 1988, Fractals (NY, USA: Plenum Press)
- Fox, D. B., Frail, D. A., Price, P. A., et al. 2005, Nature, 437, 845
- Frail, D. A., Kulkarni, S. R., Sari, R., et al. 2001, ApJ, 562, L55

F. Tamburini: Fractal – multifractal distribution – angular distribution of GRBs

- Fryer, C. L., & Kalogera, V. 2001, *ApJ*, 554, 548
- Galama, T. J., Vreeswijk, P. M., van Paradijs, J., et al. 1998, *Nature*, 395, 670
- Gehrels, N., Barthelmy, S. D., Burrows, D. N., et al. 2008, *ApJ*, 689, 1161
- Ghirlanda, G., Magliocchetti, M., Ghisellini, G., & Guzzo, L. 2006, *MNRAS*, 368, L20
- Ghirlanda, G., Nava, L., Ghisellini, L., Celotti, A., & Firmani, C. 2009, *A&A*, 496, 585
- Goltz, C. 1997, *Fractal and Chaotic Properties of Earthquakes* (Berlin: Springer-Verlag)
- Goodman, J. 1986, *ApJ*, 308, L47
- Grindlay, J., Portegies Zwart, S., & McMillan, S. 2006, *Nature Phys.*, 2, 116
- Grupe D., Burrows, D. N., Patel, S. K., et al. 2006, *ApJ*, 653, 462
- Kouveliotou, C., Meegan, C. A., Fishman, G. J., et al. 1993, *ApJ*, 413, L101K
- Kulkarni, S. R., Frail, D. A., Wieringa, M. H., et al. 1998, *Nature*, 395, 663
- Kurokawa, T., Morikawa, M., & Mouri, H. 1999, *A&A*, 344, 1
- Kurokawa, T., Morikawa, M., & Mouri, H. 2001, *A&A*, 370, 358
- Lim, S. C., & Muniandy, S. V. 2002, *Phys. Rev. E.*, 66, 021114
- Magliocchetti, M., Ghirlanda, G., & Celotti, A. 2003, *MNRAS*, 343, 255
- Mandelbrot, B. B. 1975, *Comptes Rendues (Paris)*, 280A, 1551
- Martínez, V. J., & Saar, E. 2001, *Statistics of the Galaxy Distribution* (Boca Raton: Chapman and Hall/CRC Press)
- Mészáros, A. 2006, *Rep. Prog. Phys.*, 69, 2259
- Mészáros, A., Bagoly, Z., Horváth, I., Balázs, L. G., & Vavrek, R., 2000a in *GAMMA-RAY BURSTS: 5th Huntsville Symposium*. AIPC, 526, 102
- Mészáros, A., Bagoly, Z., & Vavrek, R. 2000b, *A&A*, 354, 1
- Mészáros, A., Bagoly, Z., Horváth, I., Balázs, L. G., & Vavrek, R. 2000c, *ApJ*, 539, 98
- Metzger, B., Piro, A., & Quataert, E. 2009, *MNRAS*, 390, 781
- Mukherjee, S., Feigelson, E. D., Babu, G. J., et al. 1998, *ApJ*, 508, 314
- Narayan, R., Paczynski, B., & Piran, T. 1992, *ApJ*, 395, L83N
- Narayan, R., Piran, T., & Kumar, P. 2001, *ApJ*, 557, 949
- Nysewander, M., Fruchter, A. S., & Peer, A. 2009, *ApJ*, 701, 824
- Paczyński B. 1986, *ApJ*, 308, L43
- Paczyński B. 1990, *ApJ*, 363, 218
- Paczyński B. 1991, *Acta Astron.*, 41, 257
- Peebles, P. J. E. 1980, *The Large Scale Structure of the Universe* (Princeton University Press)
- Peebles, P. J. E. 1993, *Principles of Physical Cosmology* (Princeton Univ. Press)
- Pietronero, L. 1987, *Phys. A*, 144, 257
- Ruffini, R., et al. 2009, in *Proceedings of the 2008 Cefalù Conference*, AIPC, 1111, 325
- Salvaterra, R., Della Valle, M., Campana, S., et al. 2009, *Nature*, 461, 1258
- Soderberg, A. M., Berger, E., Kasliwal, M., et al. 2006, *ApJ*, 650, 261
- Tanvir, N. R., Chapman, R., Levan, A. J., & Priddey, R. S. 2005, *Nature*, 438, 991
- Usov V. V., & Chibisov, G. V. 1975, *SVA*, 19, 115
- van Paradijs, J. 1999, *Science*, 286, 693
- Vavrek, R., Balázs, L. G., Mészáros, A., Horváth, I., & Bagoly, Z. 2008, *MNRAS*, 391, 1741
- Wall, J. V., & Jenkins, C. R. 2003, *Practical statistics for astronomers* (Cambridge University Press)
- Wijiers, R. A. M. J., Bloom, J. S., Bagla, J. S., & Natarajan, P. 1997, *MNRAS*, 294, L13
- Woodsley, S. E. 2001, in *Gamma-Ray Bursts in the Afterglow Era*, *Proceedings of the International Workshop Held in Rome, Italy, 17–20 October 2000*, *ESO ASTROPHYSICS SYMPOSIA*, ed. E. Costa, F. Frontera, & J. Hjorth (Springer-Verlag), 257
- Zhang, B., Zhang, B.-B., Liang, E.-W., et al. 2007, *ApJ*, 655, L25